MECHANISMS OF Cs^+ BLOCKADE IN A Ca^{2+}-ACTIVATED K^+ CHANNEL FROM SMOOTH MUSCLE

XIMENA CECCHI, DANIEL WOLFF, OSVALDO ALVAREZ, AND RAMÓN LATORRE
Departmento de Biologia, Universidad de Chile, Casilla 653, Santiago, Chile, and Centro de Estudios Cientificos de Santiago, Casilla 16443, Santiago 9, Chile

ABSTRACT Large unitary conductance Ca^{2+}-activated K^+ channels from smooth muscle membrane were incorporated into phospholipid planar bilayers, and the blockade induced by internally and externally applied Cs^+ was characterized. Internal Cs^+ blockade is voltage dependent and can be explained on the basis of a Cs^+ binding to a site that senses 54% of the applied voltage, with an apparent dissociation constant, $K_d(0)$, of 70 mM. On the other hand, external Cs^+ blocks the channel in micromolar amounts, and the voltage dependence of blockade is a function of Cs^+ concentration. The fractional electrical distance can be as large as 1.4 at 10 mM Cs^+. This last result suggests that the channel behaves as a multi-ion pore. At large negative voltages the I-V relationships in the presence of external Cs^+ show an upturn, indicating relief of Cs^+ block. External Cs^+ blockade is relieved by increasing the internal K^+ concentration, but can be enhanced by increasing the external K^+. All the characteristics of external Cs^+ block can be explained by a model that incorporates a "knock-on" of Cs^+ by K^+.

INTRODUCTION

Most K^+-selective channels are blocked by Cs ions. For squid and node of Ranvier K^+ channels, it has been proposed that the narrow part of the pore has a diameter of ~0.3 nm, which is large enough to accept unhydrated K^+ (0.266 nm), but Cs^+ fails to permeate because of its size (0.338 nm). The squid axon K^+ channel can be blocked by Cs^+ from either the inner or outer end of the channel in a voltage-dependent manner, suggesting that this alkali cation can penetrate into the pore from the external or the internal solutions (Adelman and Senft, 1966; Bezanilla and Armstrong, 1972; Adelman and French, 1978; French and Shoukimas, 1985). Actually, Cs^+ can, albeit sluggishly, pass through the channel (French and Shoukimas, 1985). The characteristics of Cs^+ blockade in several potassium channels indicate that this cation can be used as a probe to distinguish between different models of ion conduction. In particular its voltage dependence shows a complex behavior with concentration of the blocking ion, and indicates that this type of channel is a multi-ion pore (Adelman and French, 1978; Hille and Schwarz, 1978).

More recently a new class of highly selective K^+ channel has been described; these channels show a large unitary conductance (~200 pS in 0.1 M KCl) and are activated by cytoplasmatic calcium (Latorre and Miller, 1983; Petersen and Maruyama, 1984; Marty, 1983; Latorre et al., 1985; Schwarz and Passow, 1983). These channels have a selectivity sequence, as determined from biionic potential of $Tl^+ > K^+ > Rb^+ > NH_4^+$; Cs^+, Na^+, and Li^+ are immeasurably permeant and they all induce a voltage-dependent blockade (Latorre et al., 1983; Latorre, 1986; Cecchi et al., 1986; Yellen, 1984*a*,*b*; Blatz and Magleby, 1984; Eisenman et al., 1986). Thus, these maxi Ca^{2+}-activated K^+ (CaK) channels show a selectivity similar to other K^+ channels, but their conductance is 20- to 100-fold larger (2 pS for the Helix neuron K^+ channel [Reuter and Stevens, 1980]; 18 pS for the squid axon channel [Conti and Neher, 1980]). We proposed a one-ion pore model that can conciliate large conductance with high selectivity for CaK channels (Latorre and Miller, 1983), but recently evidence is mounting that these types of channels are indeed multi-ion pores: (*a*) the conductance vs. concentration curve cannot be described by a one-ion pore conduction mechanism (Cecchi et al., 1986; Vergara et al., 1984; Moczydlowski et al., 1985); (*b*) increasing external K^+ relieves blockade by internal sodium by increasing the exit rate of Na^+ from the channel (Yellen, 1984*b*); and (*c*) the channel shows an "anomalous mole fraction" effect in the presence of mixtures of ions (Eisenman et al., 1986).

Yellen (1984*a*), Cecchi et al. (1984), and Wolff et al. (1985) have shown that Cs^+ can block CaK channels from the internal and the external side, and that external Cs blockade showed characteristics consistent with a multi-ion pore conduction mechanism. In this paper we have characterized in detail internal and external Cs^+ blockade. We find that much lower concentrations are required to block the channel to the same extent when Cs^+ is added to the external side. Furthermore when the external Cs^+ concentration exceeds 1 mM the voltage dependence of the block is too steep to be accounted for by the binding of a single ion per channel within the membrane electric field. We also find that although when the potassium concentration is raised at both sides of the channel the blockade is

relieved, when the K^+ is raised in the external side only the blockade is enhanced. A further series of experiments using voltage ramps indicate that, at high negative voltages, the CaK channel conductance pathway becomes permeable to Cs ions. This last result suggests that the pore wall (selectivity filter?) is somewhat deformable. We show here that these results are consistent with the behavior of multi-ion pores.

MATERIALS AND METHODS

Membrane Preparation

We used the microsomal fraction of rabbit intestinal smooth muscle prepared as described in detail by Cecchi et al. (1986). Briefly, the preparation consisted of removal of the intestine, elimination of mucosal tissue by mechanical vibration, homogenization of the remaining muscle, and differential centrifugation. The final 100,000 *g* pellet (microsomal fraction) was stored in portions of ~100 μl at −80°C.

Bilayer Formation and Channel Incorporation

Bilayers were formed from a solution containing 20 mg/ml brain phosphatidylethanolamine (PE) (Avanti Polar Lipids, Inc., Birmingham, AL) in *n*-decane (Sigma Chemical Co., St. Louis, MO). To favor fusion one of the bilayer chamber compartments was filled with a 500 mM KCl solution and the other with a 100 mM KCl solution, buffered at pH 7 with 5 mM MOPS-K. Smooth muscle membrane vesicles were added to the compartment containing the more concentrated solution. After channel incorporation, the solution can be made symmetrical either by adding KCl to the dilute compartment from a 3 M KCl solution, or by perfusing the concentrated compartment. Unlike the CaK channel from skeletal muscle, the CaK channel is inserted into the bilayer randomly. In the Results, we define the internal side as the one containing Ca^{2+} sites. Positive potentials correspond to depolarizations of the cell.

Electrical Measurements

Lipid bilayers were formed in a small hole (~200-μm diam) made in a Teflon partition (25-μm thick) that separates the two-chambered compartments. The current passing through the membrane was measured with a two-electrode voltage clamp (Alvarez and Latorre, 1978). One side of the chamber was connected to a waveform generator and the other to a current-to-voltage converter. Connections were made through Ag/AgCl electrodes connected to 1 M KCl agar bridges to minimize junction potentials. The current-to-voltage converter was a Burr-Brown OPA 111 operational amplifier (Burr-Brown Corp., Tucson, AZ) with a feedback resistor of 1 GΩ. The output of this stage was amplified to a final gain of 10 pA/V, and passed through a two-pole, low-pass active filter (model FLT-U2; Datel, Canton, MA). The damping factor was adjusted to a step response without overshoot. The cutoff frequency was adjustable from 50 Hz to 10 KHz.

Formation of the bilayer was monitored applying a rectangular pulse (10 ms in duration, 5 mV in amplitude, and at a frequency of 100 Hz) and measuring the capacitance from the amplitude of the transient capacitative current. The amplitude of this current was calibrated using a 300 pF capacitor. Bilayer capacitance ranged between 200 and 500 pF. Single channel records were obtained at constant membrane potential. Current was digitized with an eight-bit resolution and a 15-kHz sampling rate, and recorded on videotape.

Current–voltage curves were obtained using a voltage ramp method (Yellen, 1984*a*; Eisenmann et al., 1986). The ramp generator was a gated triangular wave generator. When a trigger pulse was given to the generator, the voltage swings from 0 to −150 mV. At this voltage the slope changes and the voltage increases to +150 mV. Then the slope changes again and the voltage returns to 0. The absolute value of the slope of all voltage displacements was 600 mV/s. The generator has two outputs: one is the voltage, which goes to the membrane, and the other is dV/dt, which is used to subtract capacitative current from the output of the current to the voltage converter.

To acquire a voltage–current curve we used a digital oscilloscope connected to a computer. Ramp was initiated by a command from the computer. When the voltage reaches −150 mV, the generator delivers a synchronization pulse, which is used to start the acquisition of samples of current, which are stored in the memory of the digital computer. If the curve is satisfactory, it is stored on the computer diskette for analysis. One I-V curve consists of 250 current values, with a resolution of 12 bits. Each sample was taken at 1.2-mV intervals. The sampling rate was 500 Hz, and the ramp duration was 0.5 s. The current was filtered at 500 Hz.

Raw current–voltage records were further processed using the computer. The first step was to find blank records, which are records with no channel openings. The second step was to find a record with channel openings. The contents of a blank record was then subtracted from each record with channel openings. The third step was to mark the regions of the record corresponding to an open channel, and to compute a point by point average of a set of marked records. Finally a sixth degree polynomial function was fitted to the average curve, using a nonlinear curve-fitting program. We saved the factors of the polynomial functions as descriptions of the I-V curves, to be used in further analyses.

Membrane capacitance tends to decrease during the experiment. This means that blank records taken at the beginning of the experiment cannot be used to correct for capacitative current of records taken sometime later. To minimize this error, we changed the blank record used for correction each time a blank record was found. Another potential source of error is the short closures of the channel, which may not be seen because of the bandwidth of the current measurements. This may cause an underestimation of the current, especially at high positive voltages and high calcium concentrations. The validity of the results obtained with the ramp method was checked in a narrower voltage range (±100 mV) by performing histogram analysis of the single channel current amplitudes obtained at constant holding potentials. Fig. 1 shows the blockade induced by 1 mM external Cs^+. The open circles correspond to open channel currents measured at constant holding potential, and the solid curve is the result obtained with the ramp method. Inside experimental error both methods agree reasonably well, as shown in Fig. 1. We checked that the shape of the K^+ I-V curves is not affected by the presence of Ca^{2+} at concentrations up to 100 μM. At higher Ca^{2+} concentrations, the current at high positive potentials is clearly less that in the absence of Ca^{2+}. The

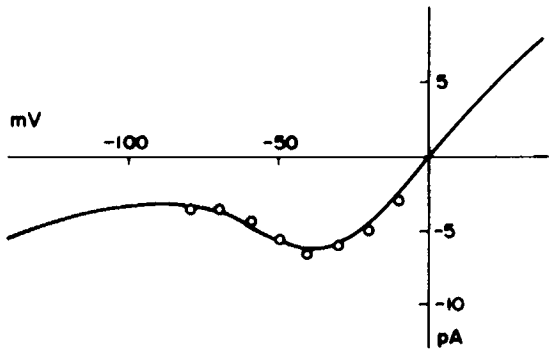

FIGURE 1 Current–voltage relationships for rabbit intestinal smooth muscle CaK channel obtained from currents measured at constant holding potential (*circles*) and using the voltage ramp method (*solid line*). The channel was incorporated to a PE lipid bilayer, and curves were obtained with 100 mM KCl, 1 mM $CaCl_2$ internal solution and 100 mM KCl, 1 mM CaCl external solution. The pH of both solutions was adjusted to 7.0 with 5 mM MOPS-K.

presence of Ca^{2+} at concentrations up to 2 mM does not influence the shape of the current–voltage relationship at negative potentials.

Calculation of I-V Curves from Barrier Models

We used a three-barrier, two-well model, allowing double occupancy, to calculate I-V curves (Cecchi et al., 1986). A state diagram was drawn, including all the possible connections of the different states of occupancy. Rate constants were stated using the peak and well energies, which are also functions of voltage and the electrical distance. A set of steady state differential equations was written using matrix notation. The probability of each occupancy state was computed using a matrix inversion procedure (Hagglund et al., 1984). Net current was then calculated. Energy of wells and peaks, and electrical distances producing the best fit to the experimental data (described as polynomial functions) were found using a nonlinear curve fitting program.

RESULTS

Block by Internal Cs^+

Cs^+ can decrease the current carried by K^+ through the CaK channel when present in the internal side (Cecchi et al., 1986). The effect of internal Cs^+ is explored here using the ramp method, over an extended voltage range. Fig. 2 *A* shows a family of I-V curves measured at different Cs^+ concentrations. We found that the effect of Cs^+ is more pronounced as voltage is made more positive. This is true for the whole voltage range. The absence of relief of the Cs^+ inhibition at high voltages suggests that this ion behaves as an impermeant blocker.

A convenient manner to represent the effect of Cs^+ is to plot the fractional reduction in K^+ current as a function of voltage, as seen in Fig. 2 *B*. For the case in which the blocker ion is competing with the permeant ion for a single site inside the channel, the ratio, i/i_o, is given by (Woodhull, 1973; Coronado and Miller, 1979)

$$i/i_o = \{1 + [Cs^+] \exp(z\delta FV/RT)/K_d(0)\}^{-1}, \qquad (1)$$

where $K_d(0)$ is the dissociation constant at zero voltage, z is the valence of the blocking ion, and δ is the fractional electrical distance at which the blocking site is located. The product $z\delta$ is usually called the effective valence of the blocking reaction (Hille and Schwarz, 1978).

We fitted all the relative current–current voltage relations determined for the different concentrations of internal Cs^+ tested using Eq. 1 (Fig. 2 *B*). The i/i_o vs. voltage curves obtained at 50 mM $[K^+]$ can be fitted with a unique $z\delta$ of 0.70 and an apparent $K_d(0)$ of 70 mM. These results are comparable with the values of 0.43 and 75 mM reported before and calculated from records of currents measured at constant holding potentials (Cecchi et al., 1986).

External Cs^+ Strongly Blocks CaK Channels

We found that external Cs^+ in micromolar amounts can reduce channel conductance, suggesting that this alkali

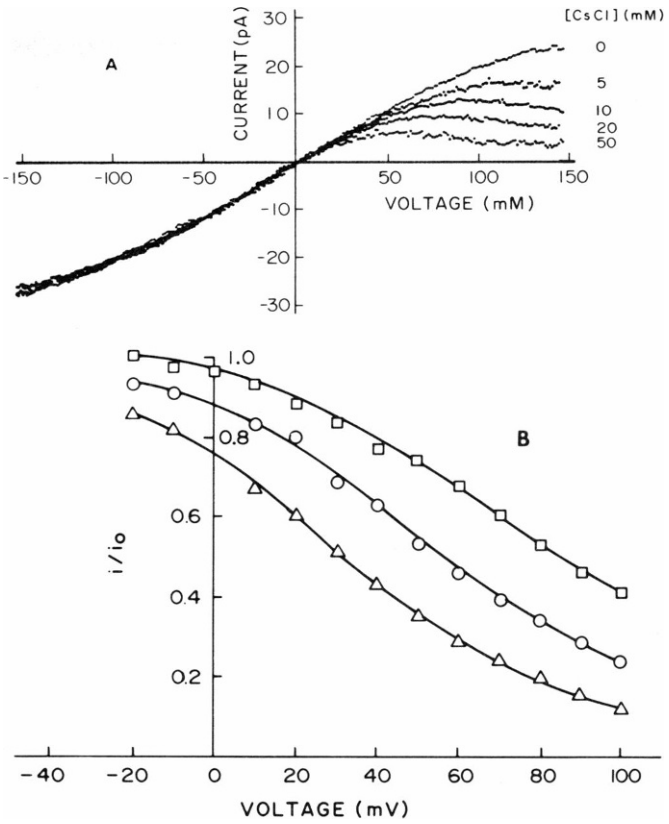

FIGURE 2 (*A*) Current–voltage relationships, showing the blockade of a single CaK channel by internal Cs^+ at concentrations of 0, 5, 10, 20, and 50 mM. Curves were obtained by using the voltage ramp method in 100 mM KCl solution buffered with 5 mM MOPS-K (pH 7). (*B*) Voltage dependence of the internal Cs^+ blockade in the CaK channel. Experimental points are the ratio between single channel currents in symmetric 50 mM KCl, 5 mM MOPS-K (pH 7), in the presence (i) and in the absence (i_o) of Cs^+ added to the internal side only at concentrations of 5, 10, and 20 mM. Solid lines represent the values of the fractional current (i/i_o) obtained by fitting Eq. 1 for a single-site blockade model to the experimental data.

cation can induce a blockade of the CaK channel. Fig. 3 *A* shows a series of I-V relationships at different Cs^+ concentrations measured by the ramp method. External Cs^+ produces a region of negative slope, and in all cases the I-V curves show an upturn at high negative voltages. French and Well (1977) found this type of behavior when studying the voltage-dependent block of the K^+ channel of the squid axon by internal sodium. More recently French and Shoukimas (1985) found the same type of shape for the "instantaneous" I-V curve for the K^+ channel when Cs^+ is present in the internal perfusate. They concluded that Cs^+ and Na^+ are forced to go through the K^+ channel at high voltages, relieving the block. We conclude that Cs^+, at high negative voltages, can go through the CaK channel, relieving the blockade.

Fig. 3 *B* shows that Eq. 1 is not a good description for the effect of external Cs^+. For voltages from 0 to −70 mV, Eq. 1 accounts for the experimental data reasonably well, but at more negative voltages clear deviations are found. It is

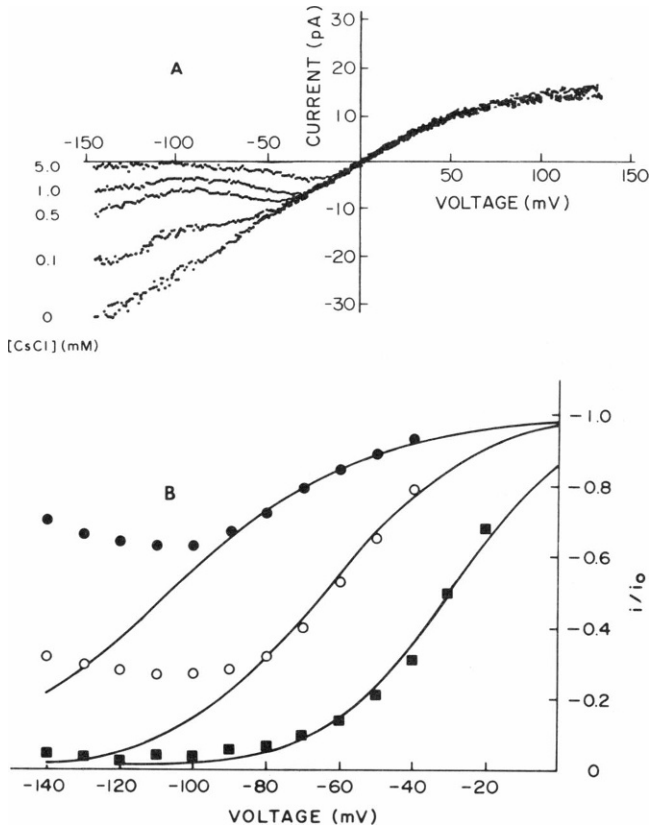

FIGURE 3 (*A*) Current–voltage relationships showing the blockade of a single CaK channel by external Cs^+ at concentrations of 0, 0.1, 0.5, 1, and 5 mM. Curves were obtained with the voltage ramp method in asymmetric 100 mM KCl solution buffered with 5 mM MOPS-K (pH 7). (*B*) Voltage dependence of the external Cs^+ blockade in the CaK channel. Experimental points are fractional currents in symmetrical 100 mM KCl, 5 mM MOPS-K (pH 7), in the presence of Cs^+ added to the external side only at concentrations of 0.1, 0.5, and 5 mM. Solid lines represent the values of the fractional current (i/i_o) obtained from a single-site blockade model in the region of voltages where data points appear to be well represented by Eq. 1.

also apparent from Fig. 3 *B* that the voltage dependence of the blockade changes with Cs^+ concentration. The blockade becomes more voltage dependent as the [Cs^+] is increased. Actually, the $z\delta$ required to fit the curves in the voltage region where Eq. 1 describes well the data were 0.93, 1.30, and 1.75 for 100, 500, and 5,000 μM Cs^+, respectively (see also Table I). An effective valence for the blocking reaction larger than 1 suggests that Cs^+ blockade of the CaK channel is a multi-ion phenomenon (Adelman and French, 1978; French and Shoukimas, 1985; Hille and Schwarz, 1978). Table I shows that the apparent dissociation constant at zero voltage is of the order of 7–20 mM, which is 3.5- to 10-fold larger than the affinity for internal Cs^+.

Cesium Carries No Detectable Current

Since the above-mentioned explanation for the upturn of the I-V curves involves the permeation of Cs^+ through the channel, we attempted to measure Cs^+ currents using pure

TABLE I
PARAMETERS OF EXTRACELLULAR Cs^+ BLOCKADE

[Cs]	$K_d(0)$	$z\delta$
mM	*mM*	
0.05	7.0	1.0
0.1	5.0	0.9
0.5	14.0	1.3
1.0	19.0	1.5
5.0	41.0	1.8
10.0	23.0	1.3

Dissociation constants of Cs^+, $K_d(0)$, and the electrical distance, $z\delta$, were calculated from Eq. 1, assuming a single site for Cs^+. Since the experimental points deviate from Eq. 1, as seen in Fig. 4, $K_d(0)$ and $z\delta$ were calculated using low negative voltages only. Voltage ranges used were: −40 to −90 mV for 0.05 mM, −40 to −90 for 0.1 mM, −40 to −80 for 0.5 mM, −40 to −70 for 1.0 mM, −20 to −60 for 5.0 mM, and −10 to −50 for 10 mM.

Cs^+ salts. In this condition no current was detected, regardless of the Cs^+ concentration used (5 mM–3 M). We also tried to measure the Cs^+/K^+ permeability ratio from zero current–voltage measurements when a membrane separates a pure K^+ solution from a pure Cs^+ solution. An I-V curve measured under this condition is in Fig. 4. The curve never crosses the voltage axis, which means that no detectable current is carried by Cs^+ and that the permeability ratio is also undetectable. This result is compatible with the hypothesis that Cs^+ blockade can be relieved by Cs^+ permeation because the movement of one Cs ion will allow the flow of many K ions. In other words, the Cs^+ current is only a minute contribution to the total current. The upturn of the I-V curves observed at high negative voltages is mainly due to K^+ current going through the CaK channel in which Cs^+ ions are forced to pass towards the internal side by the high electrochemical gradient.

Effect of Changing the K^+ Concentration

If there is competition between Cs^+ and K^+ for the same sites in the channel, the inhibition of K^+ channel currents

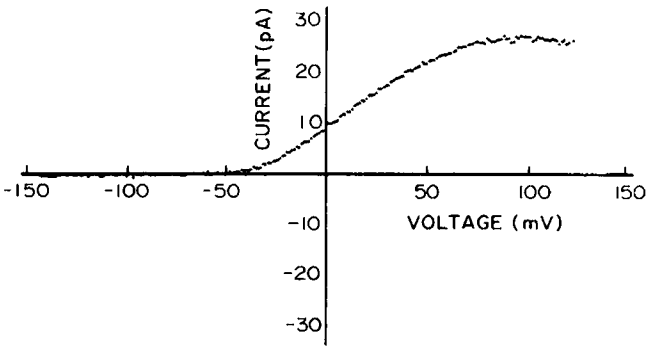

FIGURE 4 Current–voltage curve for a single CaK channel obtained under biionic conditions using the voltage ramp method. The internal side contained 400 mM KCl, 5 mM MOPS-K (pH 7), and the external side contained 100 mM CsCl, 5 mM MOPS-Cs (pH 7).

by Cs^+ should decrease with an increase in $[K^+]$. In the case of pure single-ion channels such as the K^+ channel of sarcoplasmic reticulum (SR), increasing $[K^+]$ symmetrically relieves Cs^+ block in a purely competitive fashion (Coronado and Miller, 1982). We have previously shown that when the $[K^+]$ is increased symmetrically, the Cs^+ block is relieved as if both ions were competing for the same site (Wolff et al., 1986). However, when the $[K^+]$ is increased in the external side only, the Cs^+ block shows a complex behavior. Fig. 5 *A* shows the effect of increasing the external $[K^+]$ from 100 to 200 mM. At small negative voltages, the values of i/i_o are smaller at 200 mM K^+, the difference between the two curves decreases as the voltage is made more negative, and the curves intersect each other at -70 mV. Therefore, increasing the external K^+ concentration enhances Cs^+ blockade at low voltages but relieves it at high negative voltages. On the other hand, Cs^+ block is always relieved when the $[K^+]$ concentration is increased in the internal side only (Fig. 5 *B*).

DISCUSSION

Comparison with Other K^+ Channels

Internal Cs^+ can block the K^+ channel of squid axon (Adelman and Senft, 1966; Bezanilla and Armstrong, 1972; Chandler and Meves, 1965; French and Shoukimas, 1985). In this case $z\delta$ is Cs^+ concentration-dependent, changing from 0.45 to 0.91 in the concentration range of 5–200 mM (French and Shoukimas, 1985). In this channel the apparent $K_d(0)$ is the same whether the block is induced from the internal or the external side (~750 mM), indicating a low affinity site. Internal Cs^+ also blocks the CaK channel of chromaffin cells. In this case, as in the present one, the channel has a low affinity for internal Cs^+ ($K_d(0) \sim 100$ mM; Yellen, 1984*a*). The $z\delta$ obtained for block by internal Cs^+ in chromaffin cells is 0.25. Although qualitatively the characteristics of internal Cs^+ blockade are similar to those found in chromaffin cells, the blocking parameters are different ($z\delta = 0.54$). The difference in effective valence for the blocking reaction in these two channels may suggest differences in structure of the conduction systems.

External Cs^+ blockade has been reported previously for the inward rectifier of starfish eggs and striated muscle (Hagiwara et al., 1976; Gay and Stanfield, 1977), the squid axon delayed rectifier (Bezanilla and Armstrong, 1972; Adelman and French, 1978), and the chromaffin cell CaK channel (Yellen, 1984*a*). Although the experimental conditions under which Cs^+ block was measured in chromaffin cells are not directly comparable with ours (Na was the only external cation), the voltage dependence is quite high ($z\delta \sim 1.0$). As in the squid axon, external Cs^+ blockade in CaK channels from smooth muscle is characterized by a $z\delta$ that is Cs^+ concentration dependent and can reach values larger than 1.0, indicating that CaK channels are multi-ion pores.

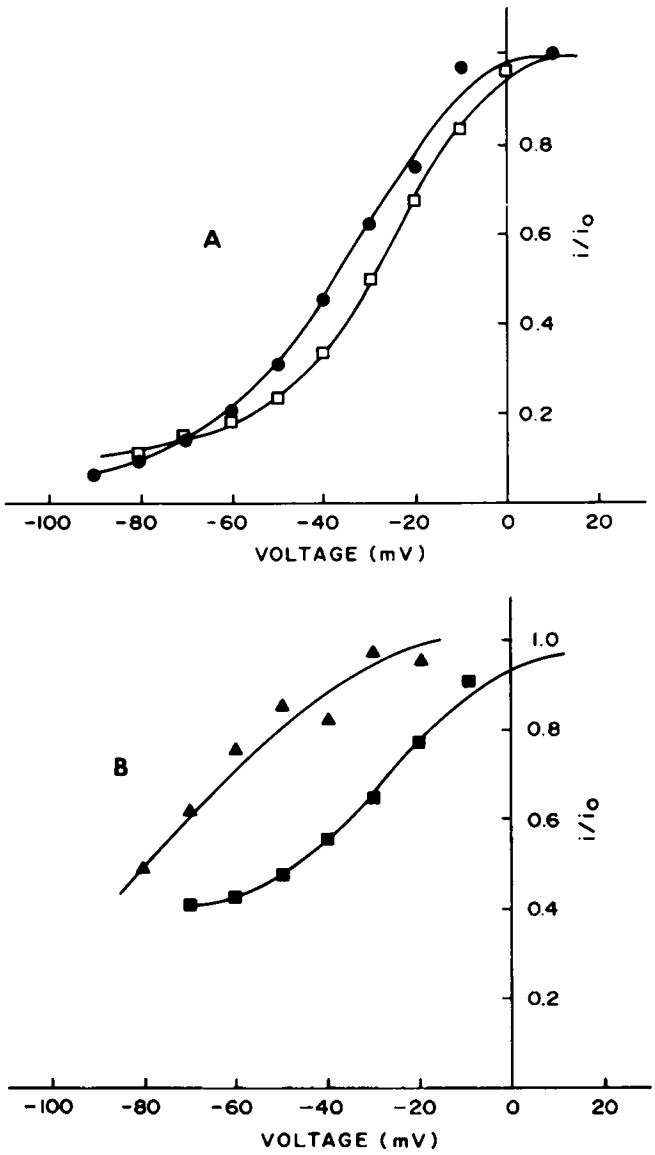

FIGURE 5 (*A*) Voltage dependence of the external Cs^+ blockade in the CaK channel, under symmetric and asymmetric K^+ solutions. Experimental points are the ratio between single channel currents in the presence (i) and in the absence (i_o) of Cs^+ added to the external side only at concentrations of 1 mM. (●) 100 mM internal K^+/100 mM external K^+; (□) 100 mM internal K^+/200 mM external K^+. (*B*) Voltage dependence of the external Cs^+ blockade in the CaK channel, under symmetric and asymmetric K^+ solutions. Experimental points are the ratio between single channel currents in the presence (i) and in the absence (i_o) of Cs^+ added to the external side only at concentrations of 1 mM. (■) 100 mM internal K^+/500 mM external K^+; (▲) 500 mM internal K^+/500 mM external K^+.

We have shown in the Results that external Cs^+ can block the CaK channel at very low concentrations. In this regard the CaK channel behaves like the anomalous rectifier of the egg cell membrane of the starfish. Strong binding of Cs^+ to the channel, combined with an energy barrier(s) high enough to oppose the passage of this alkali cation, may explain the very low permeability of Cs^+ through the CaK channel. Tight binding is expected if we

assume a K^+-selective site of low field strength in the channel (Eisenman, 1961). A site with these characteristics can bind Cs^+ more strongly than K^+.

We may compare Cs^+ blockade of the CaK channel with the Cs^+ block induced by this cation in the K^+ channel of SR (Coronado and Miller, 1979; Cukierman et al., 1985). In the SR K^+ channel the permeability (as measured by bionic potentials) of Cs^+ is almost as high as that of K^+, but its conductance is 15-fold lower than the corresponding K^+ conductance (Cukierman et al., 1985). On the other hand, Cs^+ can also induce a voltage-dependent block (Coronado and Miller, 1979). Cukierman et al. (1985) have pointed out that the high permeability of Cs^+ and its ability to block K^+ currents through the SR K^+ channel can be explained on the basis of a tight Cs^+ binding to the channel. They further argued that the rate-limiting step for Cs^+ permeation is the transit through the selectivity filter. In their barrier model the main difference between the energy profiles for K^+ and Cs^+ is given by the well depth and not by peak heights. The results showed above indicate that Cs^+ permeates very poorly through the CaK channel, but when added to the external side it can bind strongly to the channel. Despite the reservations in comparing a single ion channel (SR K^+ channel) with a multi-ion channel, it is tempting to suggest that the selectivity filter of the CaK channel is a more restrictive limiting step for ion permeation than of the SR channel. Low permeability for the CaK channel may be explained therefore by differences in both barrier heights and well depth.

Channel Blockade and Barrier Models

We have proposed a three-barrier, two-well model to explain K^+ conductance in the Ca^{2+}-activated K^+ channel of the intestinal smooth muscle (Cecchi et al., 1986). In the case of internal Cs^+ blockade, the model can be extended by adding an occupancy state, which has a Cs ion in some binding site located near the internal side. Fig. 6 *A* is a representation of the different occupancy states of the channel and their connections. Using this model, we found that Cs ions bind to a site located at an electrical distance of 0.54, whereas the corresponding binding site for K^+ is located at an electrical distance of 0.2 (Cecchi et al., 1986). That the electrical distances for K^+ and Cs^+ are different can be interpreted as evidence that these two ions bind to the channel at different places. If this is the case, we cannot obtain information about the nature of the K^+ binding site by comparison of the binding energy of these two ions. Thus, Cs^+ is not a good "probe" to characterize the K^+ binding site.

Channel blockade by external Cs^+ is still more complex because it is very voltage-dependent, and blockade is relieved at high membrane potential. To account for the experimental results we assumed that Cs^+ can enter the channel from the external side and block the channel by

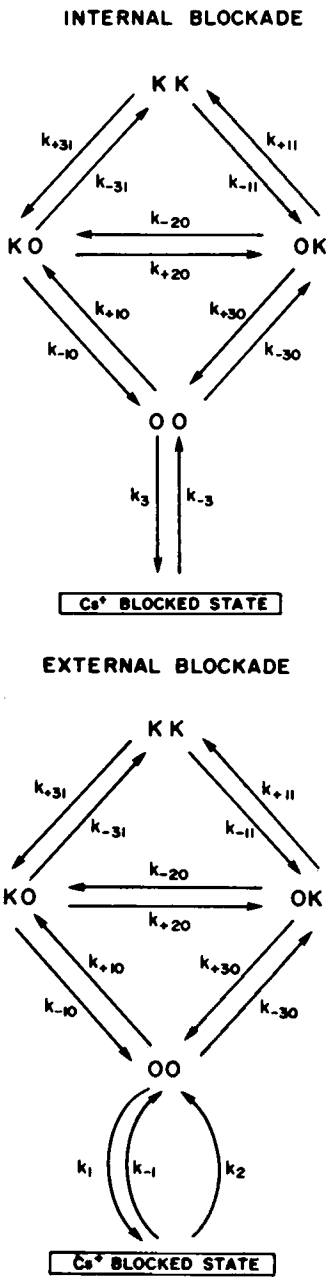

FIGURE 6 Kinetic schemes for the description of Cs^+ blockade. The upper part of each diagram corresponds to the kinetics of K^+ transport, as derived from a three-barrier, two-site model. (*A*) Kinetic diagram for internal Cs^+ blockade. The constants k^+ and k^- are for the entry of Cs^+ from the internal side and exit of Cs^+ to the internal side, respectively. (*B*) Kinetic diagram for external Cs^+ blockade. The constants, k_1 and k_{-1} corresponds to the entry of Cs^+ from the external side and exit of Cs^+ to the external side, respectively. The constant k_2 describes the exit of Cs^+ towards the internal side. The values of the different constants, found using a least square nonlinear curve fitting procedure, are

$k_{+10} = [K_i]G \exp[-(5.9 - 0.1\,U)]$
$k_{-10} = G \exp[-(11.0 + 0.1\,U)]$
$k_{+20} = G \exp[-(9.3 - 0.3\,U)]$
$k_{-20} = G \exp[-(9.3 + 0.3\,U)]$
$k_{+30} = G \exp[-(11.0 - 0.1\,U)]$
$k_{-30} = [K_0]G \exp[-(5.9 + 0.1\,U)]$
$k_{+11} = k_{+10} \exp(-12.0)$
$k_{-11} = k_{-10} \exp(+9.2)$
$k_{+31} = k_{+10} \exp(+9.2)$
$k_{-31} = k_{-10} = \exp(-12.0)$
$k_3 = [Cs_i]G \exp[-(10.8 - 0.27\,U)]$
$k_{-3} = G \exp[-(13.4 - 0.27\,U)]$
$k_1 = [Cs_0]G \exp[-(7.6 + 0.76\,U)]$
$k_{-1} = G \exp[-(14.6 - 0.76\,U)]$
$k_2 = G \exp[-(20.9 + 1.1\,U)]$.

In these expressions, U stands for the reduced potential, eV/kT, and G is a scale factor to express the ion fluxes in pA.

binding to a site. Cs^+ can leave the channel by either returning to the external solution or proceeding to the internal solution. The complete kinetic scheme is in Fig. 6 *B* and the reactions involving Cs^+ movements to and from the channel are described by the following reactions:

$$Cs_o + \text{Channel} \xrightarrow{k_1} \text{Blocked-Cs}$$

$$\text{Blocked-Cs} \xrightarrow{k_{-1}} \text{Channel} + Cs_o$$

$$\text{Blocked-Cs} \xrightarrow{k_2} \text{Channel} + Cs_i,$$

in which "Channel" refers to the empty state (state "00" in Fig 6 *B*). The probability of finding this state depends on voltage and K^+ concentration, as can be seen from the complete state diagram.

Here, Cs^+ can enter the channel from the extracellular medium and block conduction. This entry is described by a pseudo first-order kinetic constant, k_i. Cs^+ can return to the extracellular medium allowing the channel to operate again. This exit rate constant is k_{-1}. Cs^+ can also leave the channel passing towards the internal medium. The rate constant for this process is k_2. Both exit rates, k_{-1} and k_2, depend on the membrane potential in opposite ways. As membrane potential is more negative, k_{-1} decreases while k_2 increases. At low potentials Cs ions leave the channel by moving towards the external side while at high potentials it leaves passing through the channel. This will generate an N-shaped current–voltage curve, as observed in the experiments. Using the kinetic scheme of Fig. 6 *B*, we can calculate the current as a function of the kinetic constants. We can find appropriate values for the voltage-dependent rate constants k_1, k_{-1}, and k_2, which adequately describe the experimental results, with the assistance of a nonlinear curve fitting computer program. The result of the best fit is in Fig. 7.

This model can explain the shape of the I-V curves, and the apparent changes of $z\delta$ and the Cs^+ dissociation constants observed when Cs^+ concentration is varied. The

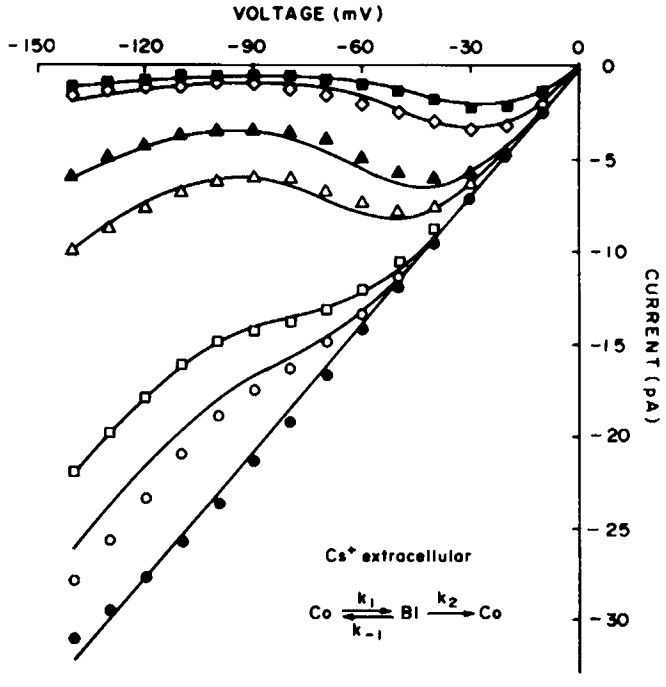

FIGURE 7 Blockade of the channel by Cs^+ from the external side. Points represent the current values obtained from experimental data shown in Fig. 3 *a*. (●) Control, 100 mM symmetric KCl; (○) 50 μM Cs^+; (□) 100 μM Cs^+; (△) 500 μM Cs^+; (▲) 1 mM Cs^+; (◇) 5 mM Cs^+, and (■) 10 mM Cs^+. The solid lines are the I-V relationships predicted by the model shown in Fig 7 *B*. Co and Bl represent the empty channel and Cs^+ blocked states, respectively.

apparent changes of these parameters arise because of the methods of determination. If Cs^+ is a nonpermeant blocker $K_d(V)$ has the form

$$K_d(V) = k_{-1}/k_1.$$

In this case the parameters $z\delta$ and $K_d(0)$ are calculated from the slope and the intercept of a plot of the logarithm of the apparent dissociation constant as a function of potential. If $K_d(V)$ is an exponential function of voltage, this plot is a straight line, and unique values of the parameters are obtained. The model we propose, on the other hand, states that the dissociation constant has the form

$$K_d(V) = (k_{-1} + k_2)/k_1.$$

In this case the kinetic constants are exponential functions of voltage, but $K_d/(V)$ need not be so. It would only be an exponential function if both k_{-1} and k_2 varied with the same voltage dependency. The slope of a plot of the logarithm of $K_d(V)$ as a function of voltage is not a straight line. The slope, $z\delta$, decreases with potential and the intercept, $K_d(0)$, also decreases as voltage is made more negative. For low values of $[Cs^+]$, the data used to calculate $z\delta$ and the dissociation constant are taken at voltages ranging from -70 to -100, while for high values of $[Cs^+]$, we used data taken from 10 to 50 mV. This explains why $z\delta$ and the dissociation constant change with $[Cs^+]$ (Table I).

The model we propose here implies that Cs^+ can pass through the channel at high negative potentials. Using the rate contants found to describe the I-V curves of Fig. 7, we can calculate the Cs^+ currents. The largest Cs^+ current, in the I-V curves of Fig. 7 is 0.37 pA at -140 mV and 10 mM Cs^+. The model predicts that the Cs^+ I-V curve has to be superlinear, and that the single channel current saturates, becoming independent of concentration above 1 mM Cs^+. The expected maximal Cs^+ currents are 0.07 pA at -100 mV and 0.38 pA at -140 mV in the absence of potassium. We attempted to measure these small Cs^+ currents in pure Cs^+ salts but we could not detect any current.

Models with multi-ion occupancy and repulsion between ions can account for the general features of the Cs^+ blockade we have found (Hille and Schwarz, 1978). For example, if the channel can be occupied simultaneously by a Cs^+ and a K^+ and Cs^+ is the first ion to enter the channel, Cs^+ exit towards the external side will be hindered by the entrance of a K^+ into the channel. Ciani et al. (1980) proposed a model of this kind to explain the voltage-dependent Cs^+ blockade of the inward rectifier of the starfish egg. The model has three barriers, two wells, and allows for double occupancy. The blocked state has Cs^+ in one internal site and K^+ in an external site. Inasmuch as the apparent electrical distance is the addition of the electrical distances of both sites, its value can be larger than one. This can be an explanation to the apparent electrical distance of 1.5 we have found for the exchange of Cs^+ with the external solution. We have to postulate a Cs^+

site located at an electrical distance $D1$ and a K^+ site located at an electrical distance $D2$, where $D1 + D2$ is 1.5.

French and Shoukimas (1985) have used an extension of the Ciani et al. (1980) model allowing Cs^+ to pass through the channel at high membrane potentials. This extension of the model is useful to explain upturn of the I-V curves we have observed at high potentials. If we assume that Cs^+ is located at a site sensing a fraction $D1$ of the applied voltage, then the voltage-dependent part of the exit rate constant will be $1 - D1$. Now we can calculate what are the maximum values of the voltage dependency of the exchange of Cs^+ and the exit rate towards the internal side. In the most favorable case the distances $D1$ and $D2$ are the same, i.e., the Cs^+ and K^+ sites are very close to each other. In this case the voltage dependency for the exchange is $2D1$. The addition of both voltage-dependent factors will be $1 - D1\ (1 - D1 + 2D1)$. The maximum value for the addition of both terms is 2, for $D1 = 1$. For the external Cs^+ blockade of the CaK channel these terms add to 2.6, exceeding the maximum value the French and Shoukimas model allows. Therefore, the two-site vacancy-diffusion model of the Eyring type cannot explain quantitatively the shape of the I-V relations shown we have found. A model of this kind, allowing more binding sites, is needed to explain our results.

A Knock-on Model

As an alternative to the vacancy models, we will use here a model involving energy transfer among the ions. The upturn of the I-V curves in the presence of external Cs^+ may arise in multi-ion channels from a knock-off process as formulated by Armstrong (1975). In this case K ions acquire enough kinetic energy to enter far enough into the channel and "knock-off" the blocking ion from the channel. Clay and Shlesinger (1983) have used this type of model to account for the external Cs^+ blockade of the squid axon delayed rectifier. As pointed out by Yellen (1984*b*), the probability that a K^+ can knock-out as a Cs^+ from its site in the channel increases linearly with K^+ concentration.

The values for the electrical distances and Cs^+ permeation in the presence of K^+ can be explained assuming that K^+ ions can push Cs^+ ions through the channel by a "knock-on" mechanism, as the one proposed by Armstrong for tetraethylammonium blockade relief by K^+ (Armstrong, 1975). In knock-on models the influence of voltage on ion conduction is very large, inasmuch as they assume that ions can be almost at the same place in the channel at the same time. Following this argument Cs^+ cannot pass through the channel if it is the only ion present in the solution, but it could permeate if K^+ is also present. The "knock-on" effect can be proved by measuring the Cs^+ kinetic constants in the presence of various K^+ concentrations. The knock-on model demands that some of these constants should depend on $[K^+]$. We have a series of experiments in which external $[K^+]$ was changed, keeping the internal $[K^+]$ constant (see Figs. 5 *A* and 8 *A*). Two features of the I-V curves obtained under these conditions can be useful to examine the effect of $[K^+]$ on the rate constants. First as extracellular $[K^+]$ increases, the position of the current maximum moves toward lower potentials (moves close to 0 mV). Second the upturn of the current occurs at lower potentials as internal $[K^+]$ increases. We first computed the I-V curves for these experimental conditions assuming that the rate constants for Cs^+ are independent of $[K^+]$. The results of these calculations are in Fig. 8 *B*. In these curves we can see that the maximum of the current moves towards higher voltages and the upturn of the current is less as $[K^+]$ increases. Both effects are in the wrong direction. If we assume now that k_1 depends on external $[K^+]$, as in Fig. 8 *C*, we see that the maximum moves in the correct direction but the upturn disappears. If we assume that k_2 also depends on extracellular $[K^+]$, both the maximum and the upturn change in the correct direction (see Fig. 8 *D*). This finding implies that both Cs^+ entry to the channel and exit towards the internal side of the channel are "knock-on" processes. Since the rate constants describing the movement of Cs^+ in the channel are proportional to K^+ concentration, we have

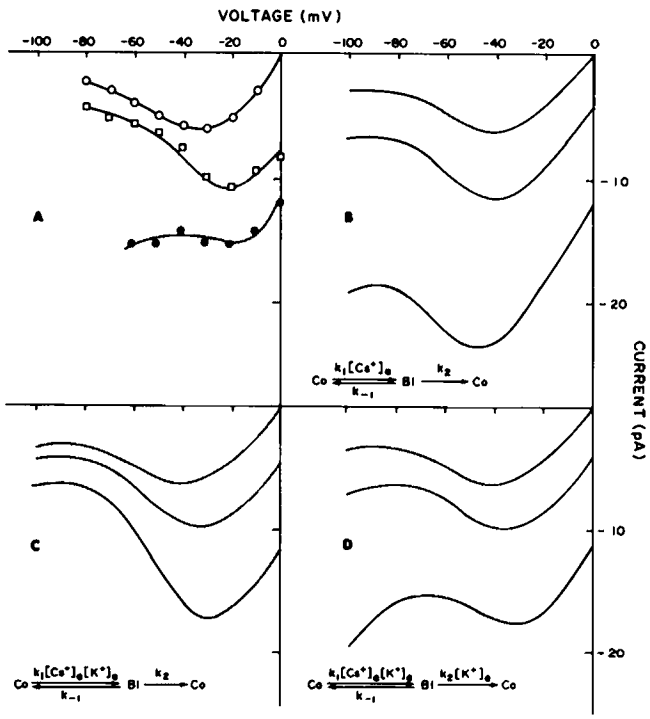

FIGURE 8 Experimental and calculated current–voltage relationships for the external Cs^+ blockade of the CaK channel, in symmetric and asymmetric K^+ solutions. (*A*) Experimental: (○) symmetric 100 mM K^+; (■) 100 internal/200 external; (●) 100 internal/500 external mM K^+. Cs^+ external concentration was 1 mM. The lines are drawn by eye. (*B*) Calculated curves with k_1 and k_2 independent on $[K^+]$. (*C*) Calculated curves with k_1 dependent and k_2 independent on $[K^+]$. (*D*) Calculated curves with k_1 and k_2 both dependent on $[K^+]$. Co and Bl represent the empty channel and Cs^+ blocked states, respectively.

to revise the prediction on the magnitude of the Cs^+ currents in the absence of potassium. The model now predicts that there must be no current in that condition. This is consistent with the observation that no Cs^+ current can be found experimentally.

A series of experiments where intracellular $[K^+]$ is varied will help us to find out if k_{-1} depends on internal $[K^+]$. The results of these experiments (Table II) tell us that there is a relief of the blockade as intracellular $[K^+]$ is increased. Using the above-discussed model, we calculated that amount of relief expected assuming that k_{-1} is independent of intracellular $[K^+]$, and we found that the relief is lower than the one obtained experimentally. Competition for the Cs^+ binding site by K^+ is not adequate to explain the degree of relief at negative voltages. If we assume that k_{-1} is proportional to internal K^+ concentration, the blockade relief is better accounted for.

The complete kinetic scheme, including the knock-off by K^+, is now

$$Cs_o + \text{Channel} + K_o \xrightarrow{k_1'} \text{Blocked-Cs} + K_i$$

$$\text{Blocked-Cs} + K_i \xrightarrow{k_{-1}'} \text{Channel} + Cs_o + K_o$$

$$\text{Blocked-Cs} + K_o \xrightarrow{k_2'} \text{Channel} + Cs_i + K_i$$

where the k' constants stand for the corresponding k constants divided by 100 mM, since the latter constants were obtained at that K^+ concentration.

A mechanistic picture can be drawn to explain the features of the model. Cs^+ can get into the channel from the external side, but it stays there for a very short time. Movement of K^+ through the channel carries along Cs ions. When the channel has a Cs^+, the K^+ flow is greatly decreased, and the channel appears to be blocked. Cs^+ cannot leave the site unless one K ion coming from the extracellular side pushes it through or a K ion coming from the internal side pushes it back. In this model there are three Cs^+ sites. One is the site seen from the internal side, and the other two are those seen from the external side. Probably vacancy models including more binding sites can also explain the results, but the number of free parameters increases enormously and the problem becomes difficult to deal with. We have chosen a knock-on type of model because of its simplicity and its ability to explain the experimental observations.

TABLE II
Cs^+ BLOCKADE RELIEF BY INCREASING INTRACELLULAR $[K^+]$

	Relative currents				
	100 mM		500 mM		
	Measured	Model 1 or 2	Measured	Model 1	Model 2
mV					
−20	0.86	0.88	0.95	0.88	0.95
−30	0.70	0.80	0.97	0.80	0.94
−40	0.56	0.68	0.82	0.70	0.90
−50	0.44	0.54	0.85	0.58	0.83
−60	0.26	0.35	0.75	0.49	0.73
−70	0.19	0.28	0.61	0.42	0.62

The figures in the table are the relative currents measured or calculated for 1 mM extracellular Cs^+, 100 mM extracellular K^+, and the indicated voltages and intracellular $[K^+]$. In model 1 it is assumed that k_2 is independent of intracellular $[K^+]$, while in model 2, k_2 is proportional to $[K^+]$. The relief of Cs^{2+} is better explained by model 2.

The authors acknowledge Dr. O. Latorre who kindly supplied the nonlinear curve fitting program, and Dr. G. Eisenman for introducing us to the voltage ramp method to measure I-V curves and to the matrix method to solve Eyring models. The able technical assistance of Mr. J. Valencia and Mr. J. Espinoza is also acknowledged.

This work was supported by Departamento de Desarrollo de la Investigación, Universidad de Chile, grant B-1985, Fondo de Nacional de Investigación, grant 1006, National Institutes of Health grant GM-35981, and by a grant from The Tinker Foundation.

Received for publication 21 July 1986 and in final form 6 January 1987.

REFERENCES

Adelman, W. J., Jr., and J. P. Senft. 1966. Voltage clamp studies on the effect of internal cesium ion on sodium and potassium currents in the squid giant axon. *J. Gen. Physiol.* 50:279–293.

Adelman, W. J., Jr., and R. J. French. 1978. Blocking of the squid axon potassium channel by external caesium ions. *J. Physiol. (Lond.).* 276:13–25.

Alvarez, O., and R. Latorre. 1978. Voltage-dependent capacitance in lipid bilayer membranes made from monolayers. *Biophys. J.* 21:1–17.

Armstrong, C. M. 1975. Potassium pores of nerve and muscle membranes. *In* Membranes: A Series of Advances. Vol. 3. G. Eisenman, editor. Marcel Dekker, New York. 325–358.

Bezanilla, F., and C. M. Armstrong. 1972. Negative conductance caused by the entry of sodium and cesium into the potassium channels of squid axons. *J. Gen. Physiol.* 60:588–608.

Blatz, A. L., and K. L. Magleby. 1984. Ion conductance and selectivity of single calcium-activated potassium channels in cultured rat muscle. *J. Gen. Physiol.* 84:1–22.

Cecchi X., O. Alvarez, and D. Wolff. 1986. Characterization of a calcium-activated potassium channel from rabbit intestinal smooth muscle incorporated into planar bilayers. *J. Membr. Biol.* 91:11–18.

Cecchi, X., Wolff, D., O. Alvarez, and R. Latorre, 1984. Incorporation of Ca^{2+}-activated channels from rabbit intestinal smooth muscle sarcolemma into planar bilayers. *Biophys. J.* 45(2, Pt. 2):38a. (Abstr.)

Chandler, W. K., and H. Meves, 1965. Voltage clamp experiments on internally perfused giant axons. *J. Physiol. (Lond).* 180:788–820.

Ciani, S., S. Krasne, and S. Hagiwara. 1980. A model for the effects of external K^+ concentration on the Cs^+ blocking of inward rectification. *Biophys. J.* 30:199–204.

Clay, J. R., and M. F. Shlensiger. 1983. Effects of external cesium and rubidium on outward potassium currents in squid axons. *Biophys. J.* 42:43–53.

Conti, F., and E. Neher. 1980. Single channel recording of K^+ currents in squid axons. *Nature (Lond.).* 285:140–143.

Coronado, R., and C. Miller. 1979. Voltage-dependent caesium blockade of a cation channel from fragmented sarcoplasmic reticulum. *Nature (Lond.).* 280:807–810.

Cukierman, S., G. Yellen, and C. Miller. 1985. The K^+ channel of sarcoplasmic reticulum: A new look at Cs^+ block. *Biophys. J.* 48:477–484.

Eisenman, G. 1961. On the elementary atomic origin of the equilibrium ion specificity. *In* Symposium on Membrane Transport and Metabolism. A. Kleinzeller and A. Kotyk, editors. Academic Press, Inc., New York. 163–179.

Eisenman, G., R. Latorre, and C. Miller. 1987. Multi-ion conduction and selectivity in the Ca^{2+}-activated K^+ channel from skeletal muscle. *Biophys. J.* 50:1025–1034.

French, R. J., and J. J. Shoukimas. 1985. An ion's view of the potassium channel: the structure of the permeation pathway as sensed by a variety of blocking ions. *J. Gen. Physiol.* 85:669–698.

French, R. J., and J. B. Well. 1977. Sodium ions as blocking agents and charge carriers in the potassium channel of the squid axon. *J. Gen. Physiol.* 70:707–724.

Gay, L. A., and P. R. Stanfield. 1977. Cs^+ causes a voltage-dependent block of inward K currents in resting skeletal muscle fibres. *Nature (Lond.).* 267:169–170.

Hagglund, J. V., G. Eisenman, and J. P. Sanblom. 1984. Single-salt behavior of a symmetrical 4-site channel with barriers at its middle and ends. *Bull. Math. Biol.* 46:41–80.

Hagiwara, S., S. Miyazaki, and N. P. Rosenthal. 1976. Potassium current and the effect of cesium on this current during anomalous rectification of the egg cell membrane of a starfish. *J. Gen. Physiol.* 67:621–638.

Hille, B., and W. Schwarz. 1978. Potassium channels as multi-ion single-file pores. *J. Gen. Physiol.* 72:409–442.

Latorre, R. 1986. The large Ca^{2+}-activated K^+ channel. *In* Ion Channel Reconstitution. C. Miller, editor. Plenum Press, New York. 431–467.

Latorre, R., O. Alvarez, X. Cecchi, and C. Vergara. 1985. Properties of reconstituted ion channels. *Annu. Rev. Biophys. Chem.* 14:79–111.

Latorre, R., and C. Miller. 1983. Conduction and selectivity in potassium channels. *J. Membr. Biol.* 71:11–30.

Latorre, R., C. Vergara, and E. Moczydlowski. 1983. Properties of a Ca^{2+}-activated K^+ channel in a reconstituted system. *Cell Calcium.* 4:343–357.

Marty, A. 1983. Ca^{2+}-dependent K^+ channels with large unitary conductance. *Trends Neurochem.* 6:262–265.

Moczydlowski, E., O. Alvarez, C. Vergara, and R. Latorre. 1985. Effect of phospholipid surface charge on the conductance and gating of a Ca^{2+}-activated K^+ channel in planar bilayers. *J. Membr. Biol.* 83:273–282.

Petersen, O. H., and Y. Maruyama. 1984. Calcium-activated potassium channels and their role in secretion. *Nature (Lond.).* 307:693–696.

Schwarz, W., and H. Passow. 1983. Ca^{2+}-activated K^+ channels in erythrocytes and excitable cells. *Annu. Rev. Physiol.* 45:359–374.

Vergara, C., E. Moczylowski, and R. Latorre. 1984. Conduction, blockade and gating in a Ca^{2+}-activated K^+ channel incorporated into planar bilayers. *Biophys. J.* 45:73–76.

Reuter, H., and C. F. Stevens. 1980. Ion conductance and selectivity of potassium channels in snail neurones. *J. Membr. Biol.* 57:103–118.

Wolff, D., X. Cecchi, D. Naranjo, O. Alvarez, and R. Latorre. 1985. Cation Selectivity and Cs^+ blockade in a Ca^{2+}-activated K^+ channel from rabbit intestinal smooth muscle. *Biophys. J.* 47(2, Pt. 2):386a. (Abstr.)

Wolff, D., C. Vergara, X. Cecchi, and R. Latorre. 1986. Characterization of a large-unitary conductance calcium-activated potassium channel in planar bilayers. *In* Ionic Channels in Cells and Model Systems. R. Latorre, editor. Plenum Press, New York. 307–322.

Woodhull, A. M. 1973. Ionic blockage of sodium channels in nerve. *J. Gen. Physiol.* 61:687–708.

Yellen, G. 1984*a*. Ionic permeation and blockade in Ca^{2+}-activated K^+ channels of bovine chromaffin cells. *J. Gen. Physiol.* 84:157–186.

Yellen, G. 1984*b*. Relief of Na^+ block of Ca^{2+}-activated K^+ channels by external cations. *J. Gen. Physiol.* 84:187–199.